Atomic-Scale Sliding Friction of Amorphous and Nanostructured SiC and Diamond Surfaces

QUERY SHEET

Tribology Transactions, 49: 1-5, 2006

ISSN: 1040-2004 print / 1547-357X online
DOI: 10.1080/05698190500486340

Atomic-Scale Sliding Friction of Amorphous and Nanostructured SiC and Diamond Surfaces

V. I. IVASHCHENKO
Institute of Problems of Materials Science
NAS of Ukraine, Krzhyzhanovsky Str. 3
03680 Kyiv, Ukraine
and
P. E. A. TURCHI
Lawrence Livermore National Laboratory (L-353)
P. O. Box 808, Livermore, CA 94551, USA

Large-scale molecular dynamics simulations are applied to the study sliding friction of a-SiC/a-SiC, a-SiC/c-C, nc-SiC/c-C and c-Si/c-C systems. The friction coefficient and structural evolution of these systems are investigated as functions of sliding velocity, temperature, and normal load. Based on our results, the physics of atomic-scale sliding friction in crystalline, nanocrystalline and amorphous materials under investigation is clarified. The established regularities are validated with available experimental results.

KEY WORDS

Friction Mechanisms; Stick-Slip Friction; Unlubricated Friction; Carbides; Diamond

INTRODUCTION

Recent advances in the deposition of carbon and silicon carbide films hold promise for producing hard protective and wear resistant coatings on a variety of substrates *(1-5)*. It becomes important to understand the friction and wear properties of such coatings. Coating surfaces are usually rough, and friction is generated between contacting asperities on the surfaces. The contact area is beyond atomic size and various friction models provide insight into the behavior within these contacts *(6, 7)*. While a few theoretical investigations of the tribological properties of crystalline diamond and silicon exist *(6,8-11)*, a theoretical understanding at the atomic-scale of sliding friction between amorphous and crystalline, amorphous and amorphous, nanocrystalline and crystalline materials is still in its infant stage. For diamond/diamond and silicon/diamond sliding pairs, friction, wear, indentation, and microstructure evolution at the sliding interface have been studied by using molecular dynamics (MD) simulations *(8–11)*. We also note that there is a growing interest in the application of MD simulations to tribology of metallic systems *(12)*.

In this paper, we carried out a series of microscopic MD simulations based on the Tersoff empirical potential *(13)* to gain insight into the physics of sliding friction of silicon-based materials. We considered the sliding of amorphous silicon carbide (a-SiC), nano-crystalline silicon carbide (nc-SiC), and crystalline silicon (c-Si) on the a-SiC and diamond (c-C) blocks. The pairs of different materials were chosen to simulate the sliding process that most often occurs in tribological experiments, for example, in ball-on-plane and polishing tests *(2-5)*. Sliding friction was investigated as a function of sliding velocity (V), temperature (T) and normal load (F_N).

METHODOLOGY

The sliding systems, analyzed in the present paper, are represented by two sliding blocks (slabs). The lower slab is associated with diamond or a-SiC, while the upper one originates from a-SiC, nc-SiC or c-Si. In experiment, heat diffuses away from the sliding interface. To simulate this effect, two reservoir regions are defined at the outer surface of the upper and lower sliding slabs. During the simulation the reservoirs are thermostated to maintain a constant low temperature. In the reservoirs, external normal (F_N) and tangential forces are applied to each atom, and the normal force is kept constant. The same tangential force applied to each reservoir is a time-dependent quantity chosen such that the average tangential velocity in the reservoir is constant, $\pm V/2$, equal and opposite in the upper and lower reservoirs. The forces are applied only to the atoms in the reservoirs. Except for the temperature control and force application, the atoms in the reservoirs are treated exactly the same as those in the remaining part of the system, and the atoms are free to enter or leave the reservoir regions. The reservoir volumes are maintained constant during MD simulations. In the corresponding experiments, the initial ball/plane contact was made when the ball is rotating, i.e., there is a relative speed between the ball and the plane. The simulation is initiated in a similar fashion. At $t = 0$, all the atoms in the upper slab are given a velocity in the positive x-direction with a magnitude equal to V/2, while all

Presented at the STLE Annual Meeting in Las Vegas, Nevada May 15-19, 2005
Manuscript approved November 16, 2005
Review led by Greg Sawyer

the atoms belonging to the lower slab are given a velocity in the negative x-direction with exactly the same magnitude, V/2. Therefore, at t=0 the relative sliding velocity of the system is V. Atoms interact with each other through the same inter-particle potentials whether they are in the reservoir or not. Since we consider sliding systems based on Si and C, the Tersoff potential is appropriate for MD simulations *(13)*. It was shown that this potential leads to correct results in many applications *(13-16)*. The selection of a proper classical potential is crucial to reproduce the real physical behavior of a system in sliding.

Prior to carrying out the simulations, sliding slabs were generated by equilibrating bulk samples with two-dimensional periodic boundary conditions for 20 ps. The a-SiC sample was generated by cooling the melt slowly from 8000 K down to 300 K *(16)*. The nc-SiC bulk sample represents the amorphous structure of a-SiC with one 3C-SiC cubic cluster with a side of 0.89 nm positioned on the lower (001) plane of the basic simulation cell. The nanocrystallite was fixed during cooling. A cooling rate of about 10^{13} K/s was chosen.

All the sliding pairs were fitted to provide the same box sizes in the x and y directions (a_x, a_y). The 506-atom upper slabs of a-SiC and nc-SiC were fitted to the 550-atom lower diamond block in a way to account for a bulk modulus (B) of 220 GPa for the upper blocks *(13)*. As a result of such a fitting, the simulation box was such that $a_x = a_y = 1.78$ nm. In the case of the c-Si/c-C sliding system, we have chosen the 576-atom diamond cluster with a $6 \times 6 \times 2$ cell in units of $a_0 = 0.356$ nm, which gives $a_x = a_y = 2.136$ nm. To fit the upper silicon slab to this size, we have chosen a $4 \times 4 \times 4$ (a_0) cluster with $a_0 = 0.534$ nm. Thus, our lattice parameter for silicon is smaller by 1.7% compared with the experimental value of 0.543 nm. Prior to sliding, both contact blocks were equilibrated during 20 ps. MD simulations of the sliding processes were carried out during 50 ps in the NVT ensemble (constant number of particles-volume-temperature). The ratio between the friction force and the normal force gives the friction coefficient μ. The average value of μ(t) was calculated after a 15 ps sliding. This time is sufficient for reaching steady-state friction. The friction coefficient of the sliding systems was calculated as a function of V, T, and F_N in the ranges of 5-800 m/s, 300-3000 K, and 0.5-5 nN, respectively.

RESULTS AND DISCUSSION

Figure 1 is a typical plot of the evolution of the friction coefficient for the systems under consideration observed in MD simulations. The friction coefficient clearly exhibits a transient overshoot before it settles down to an average steady state value. During the transient stage, the friction coefficient reaches a maximum value (μ_{max}) of about 0.5 for almost all tests. The steady sliding state is reached after about a 1.0 nm sliding. The jump of the friction coefficient during the transient stage ($\Delta\mu$) decreases in the sequence c-Si – nc-SiC – a-SiC sliding on a diamond slab. Naturally, the oscillation of the friction coefficient decreases when sliding occurs on crystalline slabs. Transient behavior in friction is commonly observed in experiments and in simulations on sliding of diamond like carbon (DLC) films *(5)*, metallic glasses *(12)*, and crystalline materials *(5, 17)*. It is believed that subsurface microstructure is created during the transient stage.

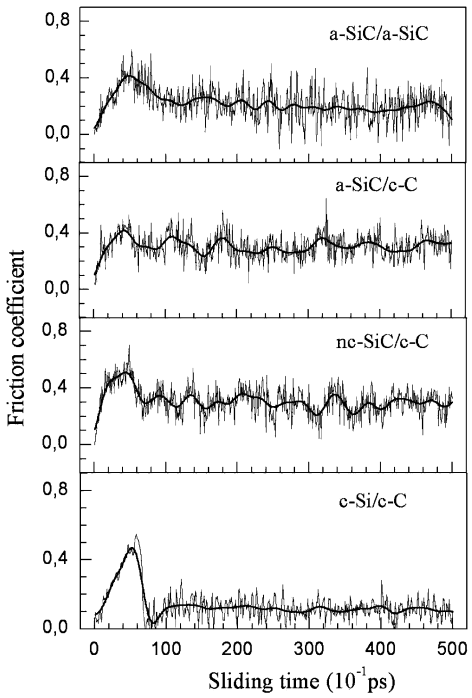

Fig. 1—Friction coefficient of a-SiC/a-SiC, a-SiC/c-C, nc-SiC/c-C and c-Si/c-C sliding systems under the following sliding conditions: V = 100 m/s, T = 300 K, and F_N = 1 nN as a function of sliding time. The solid lines correspond to an average over 25 points.

We have thoroughly investigated the microstructure of the contact zone before and after sliding. In Fig. 2 we show the atomic configurations of the a-SiC/a-SiC, a-SiC/c-C and c-Si/c-C sliding pairs at the beginning and at the end of sliding under different sliding conditions. The structure evolution of a nanocrystallite during the sliding of the nc-SiC slab on a diamond block is shown in Fig. 3. The redistribution of atoms in the z-direction after the 50 ps sliding of the a-SiC/a-SiC pair is given in Fig. 4. Based on these results and taking into account other findings on the sliding systems under consideration, we come to the following conclusions:

In the case of the c-Si/c-C sliding pairs, the lower layers of the upper block become amorphous during sliding. The c-Si/c-C friction is analogous to the one between two amorphous slabs. It should be noted that a similar amorphous layer at the surface of a silicon wafer was also revealed after sliding a diamond spherical tip on this silicon wafer *(11)*. Lattice disorder occurs mostly during the transient period, although the dynamic formation of microstructure takes place during the entire sliding time. The disordered region increases with sliding distance. The sliding plane shifts inside the silicon block, because of the strong interaction of the dangling-bond atoms of the lower silicon layers with the diamond surface atoms. These layers move together with the diamond block. No material mixing is observed at the silicon-diamond interface. The observed microstructural changes can be explained by the difference in bond strength that increases in the sequence Si-Si, Si-C and C-C. We believe that such a phenomenon is general and can be observed for other sliding hetero-pairs with different bond strengths.

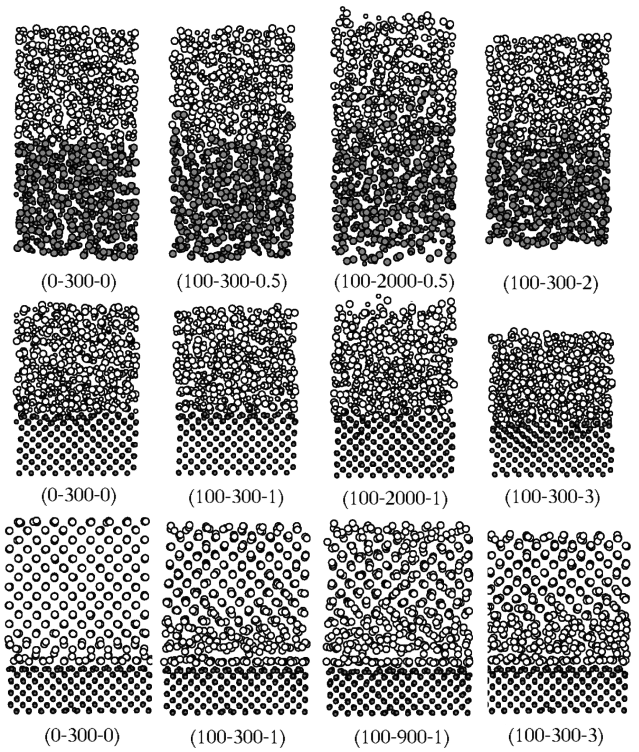

Fig. 2—Projections on the x-z plane of the atomic configuration of a-SiC/a-SiC (upper sequence), a-SiC/c-C (middle sequence) and c-Si/c-C (lower sequence) sliding systems after 50 ps simulation. Si—large open circles, C—small full circles. Only part of the carbon atoms belonging to the lower diamond slab is shown. Sample notation: (V[m/s]-T[K]-F_N[nN]). For example, the (0-300-0) systems were equilibrated prior to sliding at V = 0, T = 300 K and F_N = 0.

The sliding of the a-SiC slab on a diamond block leads to an insignificant densification of the amorphous slab. The distinct interface is preserved during sliding. No appreciable material mixing in the vicinity of the sliding interface is observed, and the adhesion of the amorphous material to the diamond surface is rather weak. One can expect that the abrasive wear of a-SiC films will be lower than that of silicon wafers, as was experimentally found in ball-on-plane tests *(3, 4)*. Adhesion wear is expected to be predominant in the c-Si/c-C sliding, despite the low friction coefficient caused by the creation of the amorphous sliding interface within the silicon block.

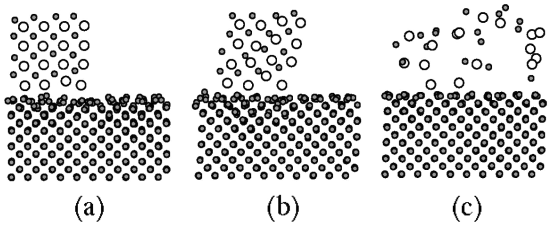

Fig. 3—Projections on the x-z plane of the atomic configuration of the nc-SiC/c-C sliding system (a,b,c) after 0, 4 ps and 50 ps simulations, respectively. The sliding conditions were V = 100 m/s, T = 300 K, and F_N = 1 nN. For the nc-SiC slab, only the nanocrystallite atoms are shown.

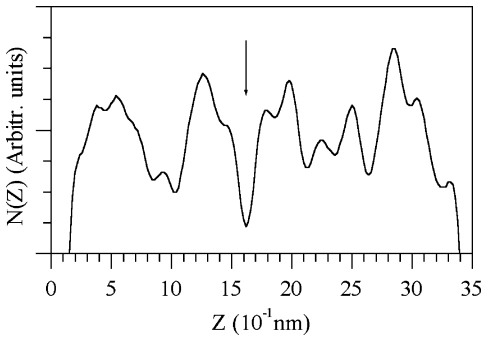

Fig. 4—Densities N(z) of the a-SiC/a-SiC sliding system after 50 ps simulation as a function of distance along the z-direction. The vertical arrow indicates the interface region with the low density. The sliding conditions: V = 800 m/s, T = 300 K, and F_N = 0.5 nN.

The character of the sliding of the nc-SiC slab on a diamond block is similar to that of the amorphous slab. However, the presence of the 3C-SiC islet slightly modifies the sliding phenomenon. In particular, the crystallite is destroyed and the crystallite atoms mix with other atoms of the amorphous block mostly during the transient stage (cf. Fig. 3).

For the a-SiC/a-SiC sliding pairs, the upper and lower blocks are chemically identical. Therefore, in the simulations, mixing was observed and the mixed layer was revealed to grow as sliding continued. The mixing of the atoms of the upper and lower blocks is mostly caused by the motion of the contacting blocks. Self-diffusion could also give rise to mixing. However, to achieve such an amount of mixing, a much longer time or a much higher temperature would be required. We note that interfacial mixing was also observed in sliding of metallic glasses *(12)*. For the a-SiC/c-C and nc-SiC/c-C sliding systems, the weak carbon diffusion towards the upper blocks is observed at the highest T, F_N and, to a lesser extent, V.

Besides these peculiarities, the a-SiC/a-SiC sliding is accompanied by the generation of a low-density region near the sliding interface at V $\geq$ 100 m/s (cf. Fig. 4). The concept of excess free volume in metallic glasses has been discussed by Spaepen and Turnbull *(18)* and Argon *(19)*. So, one can assume that the reduction in density near the sliding interface at high speed sliding is the general feature of the sliding of two non-crystalline systems.

The initially straight marked profile bends over sliding in the upper blocks. For the a-SiC/a-SiC sliding pairs, the same bent profile is observed in both slabs. For the cases considered here, the typical material flow pattern is a result of the sliding conditions that involve compression and shear. No significant profile bend in the diamond blocks has been observed in all tests. Similar profile bends were noted in corresponding experiments *(20)* and in MD simulations of the sliding of metallic glasses *(12)*.

The results on friction coefficient under various sliding conditions are summarized in Fig. 5. For all sliding pairs the steady-state friction coefficient decreases with an increase in sliding velocity, temperature, and normal load. To establish the role of temperature control on sliding, we performed simulations in the case where the temperature was controlled not only in the reservoirs but also in the entire volume of the sliding slabs. The average temperature

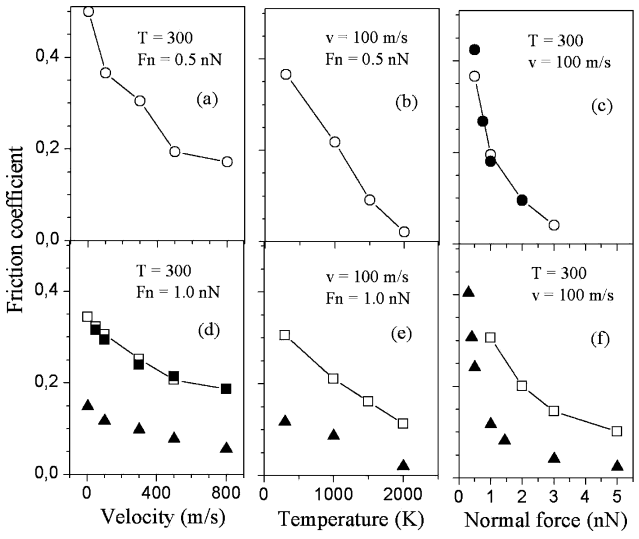

Fig. 5—Steady state friction coefficient of a-SiC/a-SiC (open circles), nc-SiC/c-C (full squares), a-SiC/c-C (open squares) and c-Si/c-C (full triangles) sliding systems after 50 ps sliding as a function of sliding velocity (V), temperature (T) and normally applied force (F_N).

of the upper block in the a-SiC/c-C sliding with V=100, 500 and 800 m/s at a constant temperature of 300 K in the reservoirs was found to increase up to 600, 1200 and 1400 K, respectively, after a 1.0 nm slide. The reduction of the temperature of the interface region to 300 K leads to a two-fold increase of μ. From this finding it follows that the thermally activated motion is responsible for the reduction in μ when the sliding velocity and the temperature of the sliding blocks increase. From our atomistic simulations the behavior of μ that depends on sliding velocity and temperature is consistent with the μ(V) and μ(T) dependencies established in experiments on c-Si and DLC film sliding *(2, 5)*.

As for the μ(P) dependence, the behavior of μ under normal load requires some explanation. In most cases of macroscopic friction, the friction force increases proportionally to the load. This relation is known as Amonton's law. According to the model that describes an experimental situation *(21)*, the contact area increases proportionally to the load in order to maintain a constant normal pressure. By assuming a specific constant shear stress of the contact, Amonton's law follows. In atomic-scale MD simulations, the contact area is a constant and the contact is established even at negative loads. Thus, the results in Fig. 5 can be interpreted in such a way that the average shear stress at the sliding interface decreases as a parabolic function of the normal pressure. We found that the temperature of the sliding interface weakly varies during sliding under various loads. This indicates that the reduction in shear stress results from a decrease in atomic-scale roughness of the sliding surfaces caused by the densification of the sliding blocks (mostly due to the densification of the disordered upper blocks). Our sliding model for the c-Si/c-C pair predicts a reduction of μ with an increase in the normal load, in agreement with the $\mu(F_N)$ dependence determined from the measurements made on Si (001) and DLC surfaces with a Si (001) ball *(2)*. In addition, there have been several studies of the effect of load on μ of diamond sliding on diamond. It has been reported that different dependencies on load are obtained for different crystal and polish orientations *(8)*. However it is difficult to compare these well known friction measurements to the results of atomistic modeling since experimentally samples are often heterogeneous over large region.

The friction coefficient obtained from the nc-SiC/c-C sliding system at low sliding velocities is slightly lower than that of the a-SiC/c-C system. The values of μ of both systems come closer with as V increases. At high speed sliding, the disappearance of the nano-crystallite is faster than at low speed sliding. The higher V is, the closer the behaviors of μ of nc-SiC to that of a-SiC are.

CONCLUSIONS

The evolution of the friction coefficient for a series of sliding systems, a-SiC/a-SiC, a-SiC/c-C, nc-SiC/c-C and c-Si/c-C, as a function of sliding velocity, temperature and normal load has been investigated. The application of the proposed model to the study of sliding friction between amorphous, nano-structured and crystalline slabs of Si, C and SiC allowed us to reproduce the main features of the sliding process observed in similar experimental setup. The suggested MD procedure is general enough to be applicable to other similar systems.

ACKNOWLEDGEMENT

This work was supported in part by the Contracts CRDF No. UK-E2-2589-KV-04 and STCU No. 1590-C. The work of P. T. was performed under the auspices of U.S. Department of Energy by the University of California Lawrence Livermore National Laboratory under Contract No. W-7405-ENG-48.

REFERENCES

(1) Yang, S., Camino, D., Jones, A. H. S. and Teer, D. G. (2000), "The Deposition and Tribological Behaviour of Sputtered Carbon Hard Coatings," *Surf. Coat. Tech.*, **124**, pp 110-116.

(2) Liu, H. and Bhushman, B. (2003), "Adhesion and Friction Studies of Microelectromechanical System/Nanoelectromechanical Systems Materials Using a Novel Microtriboapparatus." *J. Vac. Sci. Tech. A*, **21**, 4, pp 1528-1538.

(3) Esteve, J., Lousa, A., Martinez, E., Huck, H., Halac, E. B. and Reinoso, M. (2001), "Amorphous Si_xC_{1-x} Films: An Example of Materials Presenting Low Indentation Hardness and High Wear Resistance," *Diamond and Related Materials*, **10**, 3-7, pp 1053-1057.

(4) Porada, O. K., Ivashchenko, V. I., Ivashchenko, L. A., et al. (2004), "a-SiC:H Films as Perspective Wear-Resistant Coatings," *Surf. Coat. Tech.*, **180-181**, pp 121-125.

(5) Voevodin, A. A., Rebholz, C., Schneider, J. M., et al. (1995), "Wear Resistant Composite Coatings Deposited by Electron Enhanced Closed Field Unbalanced Magnetron Sputtering," *Surf. Coat. Tech.*, **73**, pp 185-197.

(6) Harrison, J. A., Stuart, S. J. and Brenner, D. W. (1999), "Atomic-Scale Simulations of Tribological and Related Phenomena," in *Handbook of Micro/Nano Tribology,* CRC Press, Boca Raton, Bhushan, B., ed., pp 525-594.

(7) Robbins, M. O. and Müser, M. H. (2000), "Computer Simulations of Friction, Lubrication and Wear," in *Handbook of Modern Tribology* CRC Press, Boca Raton, Bhushan, B., ed., pp 717-765.

(8) Hayward, I. P. (1991), "Friction and Wear Properties of Diamonds and Diamond Coatings," *Surf. Coat. Tech.*, **49**, pp 554-559.

(9) Harrison, J. A., White, C. T., Colton, C. T. and Brenner, D. W. (1992), "Molecular-Dynamics Simulations of Atomic-Scale Friction of Diamond Surfaces," *Phys. Rev. B*, **46**, pp 9700-9708.

(10) Harrison, J. A. and Brenner, D. W. (1994), "Simulated Tribochemistry: An Atomic-Scale View of the Wear of Diamond," *J. Am. Chem. Soc.*, **116**, pp 10399-10402.

(11) Zhang, L. C. and Cheong, W. C. D. (2004), "Molecular Dynamics Simulations of Phase Transformations in Monocrystalline Silicon," in *High-Pressure Surface Science and Engineering,* Dirac House, Bristol, Gogotsi, Y. and Dommich V., eds., pp 57-158.

(12) Fu, X.-Y., Falk, M. L. and Rigney, D. A. (2001), "Sliding Behavior of Metallic Glass. Part II. Computer Simulation," *Wear,* **250**, pp. 420-430.

(13) Tersoff, J. (1994), "Chemical Order in Amorphous Silicon Carbide," *Phys. Rev. B* **49**, pp 16349-16352.

(14) Kelires, P. C. (1997), "Short-Range Order, Bulk Moduli, and Physical Trends in c-$Si_{1-x}C_x$ Alloys," *Phys. Rev. B*, **55**, pp 8784-8787.

(15) Gao, F. and Weber, W. J. (2001), "Computer Simulation of Disordering and Amorphization by Si and Au Recoils in 3C-SiC," *J. Appl. Phys.*. **89**, pp 4275-4281.

(16) Ivashchenko, V. I. and Shevchenko, V. I. (2001), "Effect of Short-Range Disorder Upon Electronic Prperties of a-SiC Alloys," *Appl. Surf. Sci.*, **184**, pp 137-143.

(17) Rise, S. L., Nowothy, H. and Wayne, S. F. (1989), "A Survey of the Development of Subsurface Zones in the Wear of Materials," *Key Eng. Mater.*, **33**, pp 77-100.

(18) Spaepen, F. and Turnbull, D. (1974), "A Mechanism for the Flow and Fracture of Matallic Glasses," *Scripta Met.* **8**, pp 563-568.

(19) Argon, A. (1979), "Plastic Deformation in Metallic glasses," *Acta. Met.* **27**, pp 47-58.

(20) Heilmann, P., Don, J., Sun, T. C., et al. (1983), "Sliding Wear and Transfer," *Wear,* **91**, pp 171-190.

(21) Bowden, F. P. and Tabor, D. (1986), "*The Friction and Lubrication of Solids*," Clarendon, Oxford.